J. Phys. B: At. Mol. Opt. Phys. **23** (1990) 1655–1669. Printed in the UK

Non-local coupled-channels optical calculation of electron scattering by atomic hydrogen at 54.42 eV

K Ratnavelu† and I E McCarthy

Institute for Atomic Studies, The Flinders University of South Australia, Bedford Park, SA 5042, Australia

Received 2 November 1989

Abstract. The present study incorporates the non-local optical potentials for the continuum within the coupled-channels optical framework to study electron scattering from atomic hydrogen at 54.42 eV. Nine-state coupled-channels calculations with non-local and local continuum optical potentials were performed. The results for differential, total and ionisation cross sections as well as the 2p angular correlation parameters λ and R are comparable with other non-perturbative calculations. There are still discrepancies between theory and experiment, particularly for λ and R at larger angles.

1. Introduction

Electron scattering by atomic hydrogen is the simplest non-trivial example of electron–atom scattering processes. It is a three-body Coulomb problem consisting of a proton and two electrons. Although the two-body Coulomb problem can be solved exactly, the exact solutions to more complicated n-body Coulombic systems are impossible to obtain. The electron–hydrogen atom collision system provides an excellent testing ground for the numerous approximate theoretical methods available for electron–atom scattering. The success or failure of these methods leads us to a better understanding of the problems that are encountered in other complex collision systems.

The importance of studying this system is evident from the volume of research that has been done on it in the last thirty years. Rapid advances in experimental techniques in the early 1970s have led to measurements of the differential cross sections for both elastic and inelastic scattering of electrons by atomic hydrogen (Lloyd *et al* 1974, Williams 1974, 1975, Williams and Willis 1974, 1975, van Wingerden *et al* 1977). This stimulated much theoretical study and gave impetus to the development of sophisticated theoretical methods. Reviews of theoretical techniques are given by Burke and Williams (1977), Bransden and McDowell (1977), Byron and Joachain (1977), Henry (1981), Walters (1984) and Burke (1985). Up to now there are significant areas of discrepancy between experiments and calculations in the intermediate-energy region. This energy regime encompasses the energy range from just below the first ionisation threshold to a few (10–15) times this threshold. The recent confirmation of the measurements of Lloyd *et al* (1974), Williams (1975, 1981), Williams and

† Permanent address: Department of Mathematics, University of Malaya, Pantai Valley, 59100 Kuala Lumpur, Malaysia.

0953-4075/90/101655+15$03.50

Willis (1975) and van Wingerden *et al* (1977) by Lower *et al* (1987) suggests that the theoretical understanding of the simplest electron–atom collision system is still far from complete (Bransden *et al* 1985, Madison *et al* 1985, Byron *et al* (1985), van Wyngaarden and Walters 1986, Lower *et al* 1987, Bray *et al* 1989, Ratnavelu 1989). Hence there is evidently much still to be done in developing theoretical methods that can be used to study more complex systems (see Fon *et al* (1988) for electron–helium atom systems; Mitroy *et al* (1987) for electron–sodium atom systems; Mitroy and McCarthy (1989) and McCarthy *et al* (1989) for electron–magnesium atom systems).

The extension of traditional low-energy techniques, like the coupled-channels method, to these intermediate-energy scattering processes necessitates the explicit inclusion of the many open discrete channels as well as the continuum. The development of new reliable methods to study collision processes in this energy regime has posed a challenging task for most of the last twenty years (Burke and Webb 1970). Nevertheless, there has been considerable progress, which has resulted in the development of some sophisticated theoretical techniques. Among these methods are the pseudostate methods (Burke and Webb 1970, van Wyngaarden and Walters 1986, Callaway *et al* 1987), *R*-matrix methods (Scholz *et al* 1988) and optical potential methods (McCarthy and Stelbovics 1980, 1983, Bransden *et al* 1982, Bray *et al* 1989).

Optical potentials in electron–atom collision physics have been widely used since the early 1970s. Most of the early approaches (Winters *et al* 1974, Vanderpoorten 1975, Byron and Joachain 1974a, b), which used the closure approximation, have been reviewed by Brandsen and McDowell (1977). In recent years, the coupled-channels optical method (CCO) of McCarthy and Stelbovics (1980, 1983) has attained reasonable success in studying intermediate-energy electron scattering by atomic hydrogen (Lower *et al* 1987), by magnesium (McCarthy *et al* 1989), and by helium (McCarthy *et al* 1988).

In the present work, the CCO method of McCarthy and Stelbovics is applied to study electron scattering by atomic hydrogen at 54.42 eV. The present study attempts to incorporate the effects of the continuum by the use of *ab initio* non-local optical potentials in a coupled-channels calculation without using any equivalent local approximations. Due to the magnitude of the computational complexity, the calculations were done only at 54.42 eV, where a variety of experimental measurements incorporating most scattering parameters are available.

2. Theory and computational details

A detailed description of the CCO method to study electron–atom scattering processes is given by McCarthy and Stelbovics (1983). The implementation of the non-local continuum optical potential is detailed in Ratnavelu (1989). Here, we briefly review the essential features of the CCO method as well as the computational details of the non-local potential.

The CCO calculation involves the solution of the coupled integral equations (McCarthy and Stelbovics 1983),

$$\langle \boldsymbol{k}_i i|T|j\boldsymbol{k}_j\rangle = \langle \boldsymbol{k}_i i|V + V^{(Q)}|j\boldsymbol{k}_j\rangle + \sum_{l\in P}\int \mathrm{d}^3k\,\langle \boldsymbol{k}_i i|V + V^{(Q)}|l\boldsymbol{k}\rangle\,(E^{(+)} - \epsilon_l - \tfrac{1}{2}k^2)^{-1}\,\langle \boldsymbol{k}l|T|j\boldsymbol{k}_j\rangle \qquad (1)$$

where

$$\langle \boldsymbol{k}_i i|T|j\boldsymbol{k}_j\rangle = \langle \boldsymbol{k}_i i|V|\Psi_j^{(+)}(\boldsymbol{k}_j)\rangle$$

is the T-matrix element for the transition from $(N+1)$-electron channel state $|j\boldsymbol{k}_j\rangle$ to $|i\boldsymbol{k}_i\rangle$. The ket $|\Psi_j^{(+)}\rangle$ is the formally exact solution of the $(N+1)$-electron Schrödinger equation with total energy E for entrance channel j while ϵ_l is the energy of the N-electron target state $|l\rangle$. The first-order electron–target potential V includes the appropriate exchange operator (Stelbovics and Bransden 1989). Its dependence on the total electron spin S is not indicated explicitly since sets of equations for different S are independent. The complex polarisation operator $V^{(Q)}$ is written in Feshbach formalism as

$$V^{(Q)} = VQ\,\frac{1}{(E^{(+)} - QHQ)}\,QV \tag{2}$$

where the operators P and Q project the explicitly coupled channels and the remaining channels respectively. In principle, the effect of scattering into the set Q of the reaction channel space is contained in the non-local polarisation potential. The real and imaginary parts of the complex polarisation potential describe virtual and real excitations of the Q-space channels respectively.

In the present work we are attempting to incorporate the non-local polarisation potential into a coupled-channels calculation without resorting to any equivalent local approximations. The main drawback of incorporating the non-local potentials is the magnitude of the numerical calculation needed to evaluate all the potentials. This entails calculating the potentials $\langle \boldsymbol{q}' i|V^{(Q)}|j\boldsymbol{q}\rangle$ for all arbitrary q, q' and $\hat{\boldsymbol{q}}\cdot\hat{\boldsymbol{q}}'$ which include the off-shell terms in addition to the on-shell case. Here, a summary of the approximations and numerical techniques that are used in evaluating the polarisation for the continuum in momentum representation is given. The polarisation potentials for discrete excitations are omitted since these channels can be practically included in a calculation as reported here.

The momentum-space representation of the polarisation potential is written as

$$\begin{aligned} V_{ij}^{(Q)}(\boldsymbol{k}_i, \boldsymbol{k}_j) &= \langle \boldsymbol{k}_i i|V^{(Q)}|j\boldsymbol{k}_j\rangle \\ &= \sum_m \langle \boldsymbol{k}_i i|V|\Psi_m^{(-)}\rangle \left(E^{(+)} - E_m\right)^{-1} \langle \Psi_m^{(-)}|V|j\boldsymbol{k}_j\rangle \end{aligned} \tag{3}$$

where $\Psi_m^{(-)}$ is an exact ionisation wavefunction for ingoing-spherical-wave boundary conditions. By using the extreme screening approximation (McCarthy and Stelbovics 1980) for the target continuum, the polarisation potential becomes

$$\begin{aligned} V_{ij}^{(Q)}(\boldsymbol{k}_i, \boldsymbol{k}_j) = \int \mathrm{d}^3q \int \mathrm{d}^3q' \langle \boldsymbol{k}_i i|V|\boldsymbol{q}_>\psi^{(-)}(\boldsymbol{q}_<)\rangle \\ \times \left[E^{(+)} - \tfrac{1}{2}(q^2 + q'^2)\right]^{-1} \langle \psi^{(-)}(\boldsymbol{q}_<)\boldsymbol{q}_>|V|j\boldsymbol{k}_j\rangle. \end{aligned} \tag{4}$$

In the extreme screening approximation, the full Coulomb wave $\psi^{(-)}(\boldsymbol{q}_<)$ is used for the slower electron and a plane wave $\boldsymbol{q}_>$ for the faster one. This approximation is justified initially on the basis of the ability of the optical potential model to calculate ionisation cross sections which are in reasonable agreement with experimental data. The

total ionisation cross section is related to the polarisation potential for the continuum (McCarthy and Stelbovics 1980) by

$$\sigma_I = \left(\frac{2}{k}\right)(2\pi)^3 \text{ Im } V_{00}^{(Q)}(0), \tag{5}$$

where k is the momentum of the incident electron.

McCarthy and Stelbovics (1980) have shown that ionisation cross sections for the hydrogen atom calculated using the extreme screening approximation agree well with experimental data above 100 eV. Their theoretical ionisation cross sections also show fair agreement with experiment for energies as low as 50 eV. In table 1, the ionisation cross sections for the hydrogen atom using the present non-local model are compared with the values of McCarthy and Stelbovics (1980) and the experimental data of Fite and Brackmann (1958). The present values show excellent agreement with the previous calculation. Exchange has been taken into account by using the Bonham–Ochkur approximation (Bonham 1962, Ochkur 1964). It is found that exchange contributions to the ionisation and excitation cross sections calculated by the Bonham–Ochkur approximation are of sufficient accuracy (McCarthy and Stelbovics 1980) near the half energy shell. Far off shell this approximation is too inaccurate and exchange amplitudes have been omitted. This does not affect the imaginary polarisation potentials or the dipole contribution to the diagonal real polarisation potentials, which are the major contributors to the polarisation effects. The direct-to-exchange-ratios for the ionisation cross sections agree fairly well with the measured values of Alguard *et al* (1977).

Table 1. The ionisation cross section for hydrogen in units of πa_0^2. The column headed present contains the present non-local optical potential calculation. The next column is the local optical model calculation of McCarthy and Stelbovics (1980, 1983). The experimental data in the last column are centred on the data of Fite and Brackmann (1958). The experimental error is about 10%.

E (eV)	Present	Local	Expt
40	1.00	1.00	0.68
60	0.94	0.95	0.75
80	0.83	0.84	0.72
100	0.74	0.75	0.68
200	0.48	0.46	0.49

In equation (4), the integral that has to be evaluated for the ionisation amplitudes is the Coulomb transform for the target state i denoted as $C_i(\boldsymbol{k},\boldsymbol{p})$. This is defined as

$$C_i(\boldsymbol{k},\boldsymbol{p})\,Y_{lm}^*(\boldsymbol{p}-\boldsymbol{k}) = \int \mathrm{d}^3q\,\langle i|\boldsymbol{q}\rangle\langle \boldsymbol{k}+\boldsymbol{q}|\psi^{(+)}(\boldsymbol{p})\rangle. \tag{6}$$

It is calculated by a method due to Belkić (1984), who has derived these integrals in spherical coordinates for Slater-type and hydrogenic orbitals. The exact analytic expressions are given in terms of the Appell hypergeometric polynomials of two variables.

Given the analytical approximations for the ionisation amplitudes, all that is needed is to calculate the six-dimensional integral (4). This is done using the Diophantine multidimensional integration method (Stelbovics and Watts 1982, Conroy 1967).

3. Details of calculations

The description of the various CCO calculations is as follows.

(1) CCONL9. In this calculation the coupled-channels equations are solved for the P-space states 1s, 2s, 2p, 3s, 3p, 3d, 4s, 4p and 4d of atomic hydrogen. The optical potential $V^{(Q)}$ for Q space includes the non-local continuum polarisation potentials for the 1s–1s, 1s–2s and 2s–2s couplings. In the 1s–2p and 2p–2p couplings, which have a small effect on the cross sections, the equivalent local continuum potentials of McCarthy and Stelbovics (1980, 1983) are used.

(2) CCONLS9. This is similar to the CCONL9 calculation in all respects except for the continuum potentials included in the calculation. Only the non-local continuum potentials for the s–s couplings have been used. No continuum polarisation potentials are included in the 1s–2p and 2p–2p couplings. This calculation tests the insignificance of the 1s–2p and 2p–2p optical potentials in CCONL9.

(3) CCOL9 and CCOLS9. Here the CCO calculations are done with equivalent local continuum potentials, CCOL9 for all the s–s, s–p and p–p couplings and CCOLS9 without the s–p and p–p continuum potentials.

The main objective of this work is to incorporate the non-local off-shell continuum polarisation potentials in a practical coupled-channels calculation. Because of the magnitude of computation that is required to evaluate these potentials, a practical approach had to be implemented.

In solving the coupled Lippman–Schwinger integral equations (1), the off-shell potential matrix elements $V_{ij}^{(Q)}(\boldsymbol{k}_i, \boldsymbol{k}_j)$ need to be evaluated. This would involve evaluating $V_{ij}^{(Q)}(\boldsymbol{k}_i, \boldsymbol{k}_j)$ for arbitrary k_i, k_j and $\cos\theta$ (where θ is the angle between the two momentum vectors). To avoid this mammoth task, the continuum potentials were calculated for a finite set of $\{k_i, k_j, \cos\theta\}$. These potentials are then incorporated into a coupled-channels calculation. To obtain an optical potential for an arbitrary k_i, k_j and $\cos\theta$, a linear interpolation formula for three variables is used (Ratnavelu 1989). Inevitably, for large total angular momentum ($J > 10$), this technique fails. To avoid getting erroneous interpolated values and considering that the on-shell continuum potentials are of the order 10^{-5} or smaller for large J the non-local continuum potentials are excluded from a CCO calculation for $J > 10$.

In the CCO calculation that incorporates the non-local continuum potentials, only the continuum potentials for the 1s–1s, 1s–2s and 2s–2s couplings were treated without localisation. The 1s–2p and 2p–2p continuum potentials were treated by the angular-momentum projection (equivalent local) method of McCarthy and Stelbovics (1980). We justify this procedure by the small effect of the s–p and p–p continuum potentials in a CCO calculation (see table 2). This is reflected by comparing the total reaction, elastic and 1s–2s transition cross sections calculated by the CCONLS9 (and CCOLS9), which omits these potentials, with the CCONL9 (and CCOL9). There is only a discernible difference of 1% between these calculations. The 1s–2p transition cross sections are also affected by only about 5–6%. In view of the small effect of omitting these potentials altogether, we are confident that the error made by using the equivalent local form will be small.

Differential and total cross sections for elastic and inelastic scattering in the 1s, 2s and 2p states, the total reaction cross section and the angular correlation parameters λ and R for the 2p state are calculated using the T-matrix elements (1). The numerical techniques used to solve the coupled integral equations are described by McCarthy and Stelbovics (1983). Here, a brief discussion of the numerical analysis is presented.

Table 2. Total elastic, inelastic, reaction and ionisation cross sections (in a_0^2) for 54.42 eV e–H elastic scattering. CCOM denotes the CCO calculation of Lower *et al* (1987). MPCC denotes the multi-pseudostate close-coupling calculation of van Wyngaarden and Walters (1986). Figures in parentheses indicate the error in the last significant digits.

	Expt	CCONL9	CCONLS9	CCOL9	CCOLS9	CCOM	MPCC
σ_{1s}	3.83[a]	3.114	3.115	3.279	3.285	3.270	3.110[f]
σ_{2s}	0.176(16)[b,d]	0.199	0.195	0.228	0.227	0.224	0.205
σ_{2p}	2.79(24)[c]	2.404	2.543	2.458	2.619	2.512	2.320
	2.261(94)[d]						
σ_{ion}	2.29[e]	2.890	2.967	3.096	3.101	3.251	
	2.42[a]						
σ_R	6.57[a]	6.391	6.328	6.682	6.569	6.620	

[a] de Heer *et al* (1977).
[b] Kauppila *et al* (1970).
[c] Williams (1981).
[d] van Wyngaarden and Walters (1986).
[e] Fite and Brackmann (1958).
[f] Walters (1988).

A 24-point Gaussian quadrature mesh is used to discretise the off-shell part of the integral equations for total angular momentum $J \leq 24$. Numerical accuracy of the order 1% is obtained with 24-point quadratures (McCarthy and Stelbovics 1983). For $J > 16$, exchange first-order potential matrix elements are negligible and are excluded. The unitarised Born approximation is used to approximate the T-matrix elements for $J > 24$. This approximation is used up to $J = 80$, where the Born approximation is sufficiently accurate. Higher partial waves are treated by the analytic Born approximation.

4. Results and discussion

4.1. Elastic scattering

The total and differential cross sections for elastic scattering, calculated by the present theory, are given in tables 2 and 3 respectively. The previous theoretical CCO calculation (CCOM) of Lower *et al* (1987) is also given. The present results are compared with the absolute measurements of Williams (1975) in figure 1. These measurements were made at 50 eV for the angular range 10–140° (see table 3).

The present calculations compare fairly well with the experiment for small- and medium-angle (up to 80°) elastic scattering but for larger angles they tend to underestimate the cross sections by 10–20%. The effect of incorporating the non-local polarisation potentials (CCONL9) lowers the elastic total cross section by 5% in comparison to the CCOL9 calculation. The use of local continuum potentials for 1s–2p and 2p–2p in the CCONL9 model has not much significant effect on the total elastic cross section. This is also reflected in the CCOL9 calculation. In comparing the CCOL9 and CCONL9 differential cross sections, there are perceptible differences. In the 20–40° angular range, the CCONL9 cross sections are about 2–4% lower, while at larger angles, the CCONL9 values lie closer to the experimental data.

The previous CCO calculation (CCOM) of Lower *et al* (1987) is nearly identical to the present CCOL9 values except for a slight difference at the forward angles (3–5% lower).

Table 3. Differential cross sections (in $a_0^2\,sr^{-1}$) for 54.42 eV e–H elastic scattering. CCOM denotes the CCO calculation of Lower *et al* (1987). Exponential notation is used. Experimental measurements are due to Williams (1975) at 50 eV. Figures in parentheses indicate the error in the last significant digits.

θ (deg)	CCONL9	CCOL9	CCOM	Expt[a]
0	8.10	7.86	7.62	
10	3.88	3.96	3.87	5.04(51)
20	1.59	1.80	1.78	2.17(23)
30	7.76–1	9.03–1	9.16–1	1.12(12)
40	4.87–1	5.18–1	5.22–1	5.51(59)–1
60	1.81–1	1.83–1	1.86–1	2.05(19)–1
80	8.53–2	8.05–2	8.03–2	9.93(121)–2
100	4.39–2	4.22–2	4.34–2	5.58(66)–2
120	2.80–2	2.59–2	2.67–2	3.49(33)–2
140	2.08–2	1.86–2	1.89–2	2.73(26)–2

[a] 50 eV.

In table 2, the total elastic cross section predicted by the multi-pseudostate coupled-channels (MPCC) calculation of van Wyngaarden and Walters (1986) is also given. The MPCC and CCONL9 cross sections are nearly identical.

In table 4, the present elastic partial-wave cross sections for the first three partial waves are compared with the recent R-matrix calculation of Scholz *et al* (1988). CCONL9 shows fairly good agreement with their cross sections.

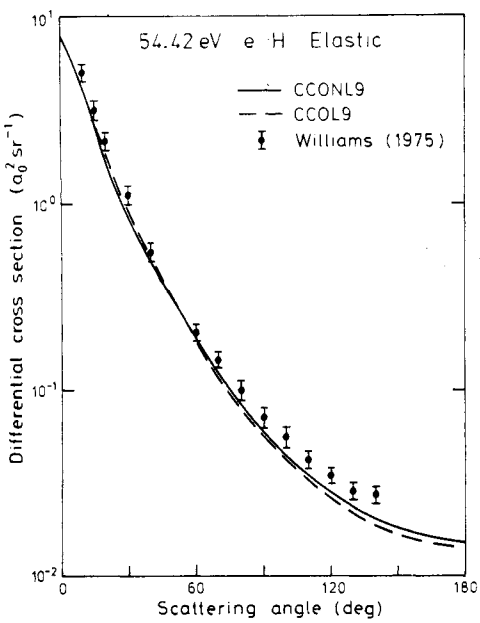

Figure 1. e–H elastic scattering at 54.42 eV. Full circles: Williams (1975), full curve: CCONL9, broken curve: CCOL9.

4.2. 2s excitation

The total and differential cross sections for the electron impact excitation of the 2s state in atomic hydrogen, calculated using the present methods, are given in tables 2 and 5 respectively. The CCOM and MPCC cross sections are also given for comparison. The absolute differential cross section measurements of Williams (1981) are illustrated in figure 2 together with some of the theoretical results. Only Williams' (1981) cross sections deduced from the ratio $\sigma(2s)/\sigma(2p)$ are shown (see table 5).

Table 4. Elastic and inelastic ($n = 2$) partial-wave cross sections for electron scattering from hydrogen at 54.42 eV in units of πa_0^2. Values include spin weighting. Exponential notation is used for the power of 10. SSB denotes the R-matrix calculation of Scholz *et al* (1988). The other notations denote the calculations described in section 3.

		SSB	CCONL9	CCOL9
Elastic	^{1}S	6.68–2	6.08–2	6.01–2
	^{3}S	4.03–1	4.14–1	4.16–1
	^{1}P	2.52–2	2.57–2	3.44–2
	^{3}P	2.71–1	2.91–1	3.19–1
	^{1}D	1.47–2	1.31–2	1.66–2
	^{3}D	8.30–2	9.63–2	1.08–1
1s–2s	^{1}S	2.79–3	2.86–3	2.96–3
	^{3}S	2.19–3	1.66–3	1.88–3
	^{1}P	7.75–3	8.91–3	9.45–3
	^{3}P	1.00–2	8.79–3	9.42–3
	^{1}D	3.69–3	4.36–3	5.12–3
	^{3}D	1.23–2	1.12–2	1.25–2
1s–2p	^{1}S	3.07–3	2.39–3	2.23–3
	^{3}S	5.23–3	4.11–3	4.17–3
	^{1}P	4.09–3	1.66–3	1.75–3
	^{3}P	5.04–3	2.61–3	2.96–3
	^{1}D	1.21–2	1.03–2	1.04–2
	^{3}D	1.40–2	1.03–2	1.11–2

The immediate observation from figure 2 is the lower backward-angle cross sections predicted by the CCONL9 and CCOL9 approximations. The CCONL9 calculation also predicts a lower forward peak than the CCOL9 and the related CCOM calculation (see table 5). The present calculations show a trend similar to that observed by the distorted-wave second Born approximation (DWSBA) of Kingston and Walters (1980), the ten-state close-coupling calculation of Edmunds *et al* (1983) and the MPCC, in predicting lower cross sections for large-angle scattering than the simple three-state close-coupling (CC3) calculation of Kingston *et al* (1976).

The present total cross sections for 2s excitation are compared with the CCOM, MPCC and experimental cross sections in table 2. The CCONL9 and MPCC cross sections are in excellent agreement with each other. The effect of using localised approximations for the continuum potentials tends to enhance the cross sections as evidenced by CCOL9 and CCOM values. The experimental value given in table 2 is from the data of Kauppila *et al* (1970) which have been corrected for cascade contributions and normalised to the MPCC cross sections at 200 eV (see van Wyngaarden and Walters (1986) for a detailed discussion). The increasingly sophisticated CCO calculations – CCOM, CCOL9

Table 5. Differential cross sections (in $a_0^2\,sr^{-1}$) for 2s excitation of hydrogen at 54.42 eV. MPCC denotes the multi-pseudostate close-coupling calculation of van Wyngaarden and Walters (1986). Experimental measurements are due to Williams (1981). Figures in parentheses indicate the error in the last significant digits.

θ (deg)	CCONL9	CCOL9	CCOM	MPCC	Expt
0	2.06	2.33	2.41	1.85	
10	3.71–1	4.47–1	4.21–1	3.93–1	5.94(94)–1
20	8.12–2	9.56–2	1.03–1	1.03–1	1.16(17)–1
30	3.18–2	3.22–2	2.67–2	2.72–2	3.75(40)–2
40	1.12–2	1.16–2	1.19–2	9.97–3	1.84(47)–2
60	5.71–3	6.59–3	6.88–3	6.28–3	1.06(31)–2
80	4.08–3	4.45–3	3.91–3	4.59–3[a]	5.27(163)–3
100	2.38–3	2.27–3	2.47–3	3.22–3[b]	3.85(129)–3
120	1.59–3	1.54–3	1.67–3	1.58–3	3.21(114)–3
140	1.10–3	1.30–3	1.25–3	1.18–3	2.24(87)–3

[a] 75°.
[b] 90°.

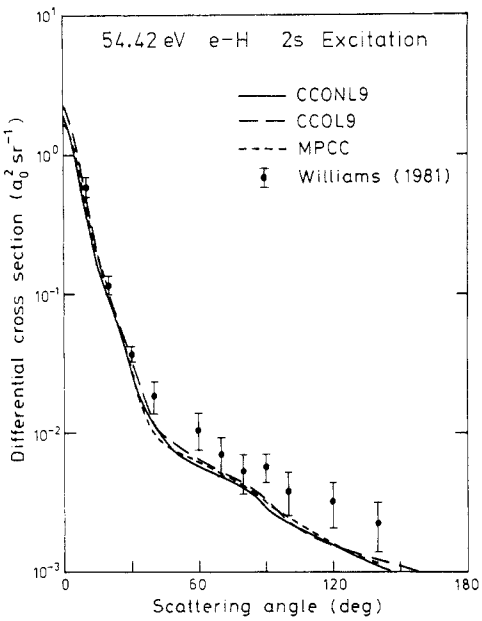

Figure 2. e–H scattering to the 2s state at 54.42 eV. Full circles: Williams (1981), full curve: CCONL9, long-dashed broken curve: CCOL9, short-dashed curve: MPCC.

and CCONL9 – are showing a trend in converging to the cross section of Kauppila *et al* (0.176 a_0^2) rather than to the value of 0.25 a_0^2 obtained by interpolation in the data of Williams (1981). There is good agreement between the CCONL9 and MPCC cross sections.

The partial-wave cross sections calculated by CCONL9 show fairly good agreement with the extensive *R*-matrix calculation of Scholz *et al* (1988) (see table 4).

4.3. 2p excitation

The present differential cross sections are given in table 6, together with relevant theoretical calculations as well as the absolute experimental measurements of Williams (1981). They are also illustrated in figure 3.

Table 6. Differential cross sections (in $a_0^2\,sr^{-1}$) for 2p excitation of hydrogen at 54.42 eV. Experimental measurements are due to Williams (1981). Figures in parentheses indicate the error in the last significant digits.

θ (deg)	CCO9NL	CCO9L	CCOM	MPCC	Expt
0	36.5	37.1	38.0	37.4	
10	6.61	6.76	6.90	6.51	7.54(71)
20	8.78–1	9.01–1	9.17–1	7.02–1	1.04(11)
30	1.36–1	1.42–1	1.44–2	9.89–2	1.57(21)–1
40	3.29–2	3.55–2	3.87–2	3.15–2	4.36(69)–2
60	7.39–3	8.10–3	8.29–3	9.59–3	1.19(21)–2
80	3.87–3	3.90–3	3.85–3	4.69–3[a]	4.05(87)–3
100	2.19–2	2.13–3	2.11–3	2.57–3[b]	2.16(46)–3
120	1.31–3	1.17–3	1.33–3	1.01–3	1.59(36)–3
140	1.00–3	1.03–3	9.45–3	8.10–4	1.03(28)–3

[a] 75°
[b] 90°

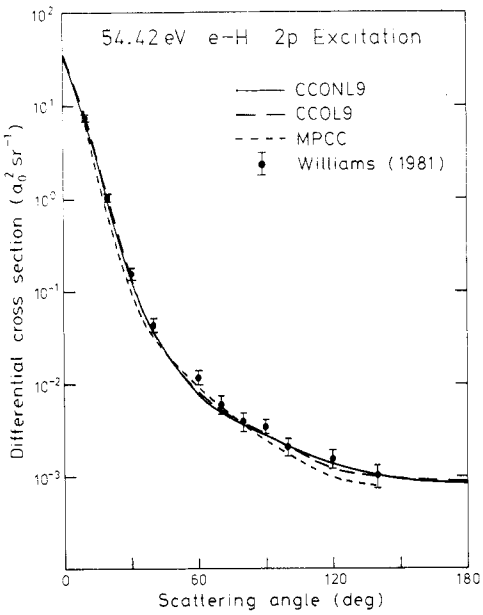

Figure 3. e–H scattering to the 2p state at 54.42 eV. Details as for figure 2.

In general, the present calculations show excellent agreement with experimental data for most scattering angles except at 60 and 90°, where the theoretical values are slightly lower than the experiment. In comparison, the MPCC calculation shows only

reasonable agreement with experiment up to 100° and underestimates the large-angle cross sections.

The total cross sections for 2p excitation calculated using the present methods and other theories are given in table 2. The present numbers are in good agreement with the experimental data of Long *et al* (1968), which were normalised to the MPCC calculation at 200 eV (van Wyngaarden and Walters 1986). The CCONL9 and CCOL9 cross sections are smaller than the previous CCOM calculation of Lower *et al* (1987). The MPCC and CCONL9 cross sections are in good agreement.

The partial-wave cross sections are compared with the *R*-matrix cross sections (Scholz *et al* 1988) in table 3. Except for the P-wave cross sections, where CCOL9 and CCONL9 are substantially smaller, there is fair agreement.

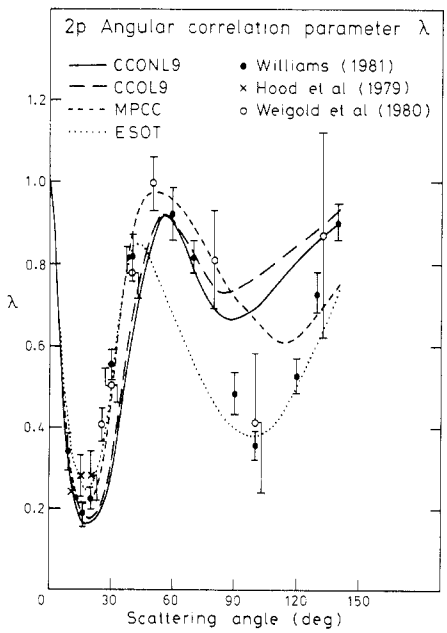

Figure 4. λ correlation parameter. Details as for figure 2 with crosses: Hood *et al* (1979), open circles: Weigold *et al* (1980), dotted curve: ESOT.

4.4. Angular correlation parameters

The angular correlation parameters λ and R measured by Hood *et al* (1979) for angles 10–20°, Weigold *et al* (1980) for angles 25–133° and Williams (1981) for angles 10–140° are shown in figures 4 and 5 respectively. Present theoretical calculations together with the MPCC and the explicit second-order theory (ESOT) of Madison *et al* (1985) are also shown. Theoretical and experimental (Williams 1981) numbers for λ and R are given in tables 7 and 8 respectively.

The main feature of the attempts to describe λ is that no calculation is good over the whole angular range. CCONL9 and CCOL9 are rather similar, being significantly too low in the 30° region and having a backward minimum that is too shallow. They give a significantly worse description than MPCC, where the backward minimum is the only difficulty. ESOT corrects the backward deficiency at the expense of the 50° maximum.

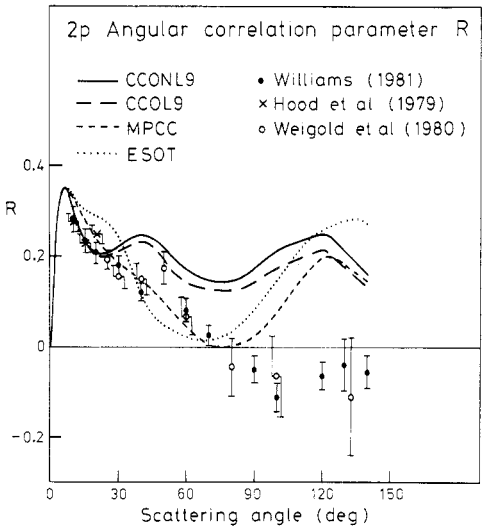

Figure 5. *R* correlation parameter. Details as for figure 4.

Table 7. 2p angular correlation parameter λ for 54.42 eV e–H scattering. Experimental measurements are due to Williams (1981). Figures in parentheses indicate the error in the last significant digits.

θ (deg)	CCONL9	CCOL9	CCOM	MPCC	Expt
0	1.00	1.00	1.00	1.00	
10	0.26	0.28	0.28	0.31	0.34(5)
20	0.16	0.17	0.17	0.22	0.23(3)
30	0.29	0.31	0.32	0.49	0.55(4)
40	0.63	0.67	0.66	0.88	0.82(6)
60	0.89	0.91	0.91	0.96	0.92(6)
80	0.68	0.74	0.75	0.85[a]	
100	0.70	0.77	0.74	0.72[b]	0.35(3)
120	0.74	0.79	0.83	0.62	0.53(4)
140	0.92	0.93	0.92	0.75	0.90(4)

[a] 75°.
[b] 90°.

The present CCO calculations show good agreement with experiment for R in the angular range 10–20°. A similar shoulder to that observed by CCOM and CC3 calculations develops in the 20–40° region. For $\theta > 50°$, the CCO calculations are overestimating the magnitude of R. In comparison, MPCC shows fair agreement with experiment up to 80°. A broad minimum at around 65–80° is predicted by all the theories shown. For $\theta > 80°$, all theories predict positive R values which is in complete disagreement with the negative R values observed by experiment. In particular, near 120°, the CCONL9, CCOL9 and MPCC give a positive maximum at odds with the opposite negative minimum observed.

In general MPCC gives a significantly better description of λ and R up to 80° than either CCO calculation. This contrasts with the differential cross section for the

Table 8. 2p angular correlation parameter R for 54.52 eV e–H scattering. Experimental measurements are due to Williams (1981). Figures in parentheses indicate the error in the last significant digits.

θ (deg)	CCONL9	CCOL9	CCOM	MPCC	Expt
0	0.000	0.000	0.000	0.000	
10	0.296	0.298	0.299	0.320	0.28(3)
20	0.206	0.206	0.202	0.233	0.21(2)
30	0.221	0.211	0.205	0.183	0.18(2)
40	0.247	0.233	0.238	0.150	0.122(18)
60	0.168	0.140	0.134	0.047	0.082(3)
80	0.144	0.125	0.135	−0.006[a]	
100	0.217	0.175	0.181	0.021[b]	−0.113(33)
120	0.248	0.216	0.187	0.197	−0.065(30)
140	0.164	0.136	0.146	0.148	−0.056(40)

[a] 75°
[b] 90°

same transition, where the reverse applies. Note that the logarithmic scale of figure 3 de-emphasises differences. The exchange term in the CCO polarisation potential is calculated in a much worse approximation than the direct term. This may account for the poor description of λ and R.

5. Summary and conclusions

The present calculation CCONL9 is the most detailed implementation of the CCO method to date. The direct term in each polarisation potential matrix element is a good numerical approximation to the basic approximation, which represents the three-body continuum wavefunction by the product of a plane wave for the faster electron and a Coulomb wave for the slower. The exchange term still requires the Bonham–Ochkur approximation, which is not very good for details of amplitudes, particularly off shell, but does not cause serious errors overall when integrated over on-shell kinematic variables (McCarthy *et al* 1981).

The advantage over previous implementations of CCO (e.g. CCOL9) is that the restriction to half-on-shell momenta and the angular momentum projection onto the absolute difference of the momentum coordinates (equivalent local approximation) has been removed. Since the half-on-shell calculation is much easier it is pleasing to see that differences between CCONL9 and CCOL9 are small.

The CCO calculations predict Q-space-related quantities such as total reaction and ionisation cross sections. The calculated reaction cross section lies within the experimental error limits given by de Heer *et al* (1977). Furthermore the calculated ionisation cross section is showing a fairly good agreement with the measurement of Fite and Brackmann (1958). This justifies the present simple treatment of the continuum at 54.42 eV.

The calculation has been compared mainly with another coupled-channels calculation, that of van Wyngaarden and Walters (1986) (MPCC), which represents higher discrete states and the continuum by a large set of pseudostates chosen to give a good description of the second Born integral. Partial-wave cross sections have been compared with the large intermediate-energy R-matrix calculation of Scholz *et al* (1988),

with which there is quite good agreement in the s channels but not so good in the 2p channel.

In comparison with experimental data CCONL9 tends in general towards the results of MPCC and away from less detailed CCO calculations. The 2p channel provides an interesting inconsistency in the comparison with MPCC. CCONL9 describes differential cross sections much better than MPCC, but is much worse for the electron–photon correlation parameters λ and R. In comparison with experiment CCONL9 is perhaps closer to the calculation of Byron *et al* (1985), who used the unitarised eikonal-Born series, than to MPCC. However, considering their entirely different approaches, there is significant agreement between calculations.

The worst feature of the present calculation is probably the treatment of exchange in the polarisation potential. Full partial-wave calculations (Bray *et al* 1990), where exchange is treated exactly, are expected to give a general improvement, particularly for λ and R.

Acknowledgments

One of us (KR) acknowledges a Flinders University Research Scholarship. We would like to thank Dr Jim Mitroy for many useful discussions.

References

Alguard M J, Hughes V S, Lubell M S and Wainwright P F 1977 *Phys. Rev. Lett.* **39** 344
Belkić Dž 1984 *J. Phys. B: At. Mol. Phys.* **17** 3629
Bonham R A 1962 *J. Chem. Phys.* **36** 3260
Bransden B H, McCarthy I E, Mitroy J D and Stelbovics A T 1985 *Phys. Rev.* A **32** 166
Bransden B H and McDowell M R C 1977 *Phys. Rep.* **30** 207
Bransden B H, Scott T, Shingal R and Roychoudhury R K 1982 *J. Phys. B: At. Mol. Phys.* **15** 4605
Bray I, Madison D H and McCarthy I E 1989 *Phys. Rev.* A **40** 2820
Bray I, Madison D H and McCarthy I E 1990 to be published
Burke P G 1985 in *Fundamental Processes in Atomic Collision Physics* ed H Kleinpoppen, J S Briggs and H O Lutz (New York: Plenum Press) p 51
Burke P G and Webb T G 1970 *J. Phys. B: At. Mol. Phys.* **3** L131
Burke P G and Williams J F 1977 *Phys. Rev.* A **9** 2599
Byron F W Jr and Joachain C J 1974a *Phys. Rev.* A **9** 2599
—— 1974b *Phys. Lett.* **49A** 306
—— 1977 *Phys. Rep.* **34** 233
Byron F W Jr, Joachain C J and Potvliege R M 1985 *J. Phys. B: At. Mol. Phys.* **18** 1637
Callaway J, Unnikrishnan K and Oza D H 1987 *Phys. Rev.* A **36** 2576
Conroy H 1967 *J. Chem. Phys.* **47** 5307
de Heer F J, McDowell M R C and Wagenaar J 1977 *J. Phys. B: At. Mol. Phys.* **10** 1945
Edmunds P W, McDowell M R C and Morgan L A 1983 *J. Phys. B: At. Mol. Phys.* **16** 2553
Fite W L and Brackmann R T 1958 *Phys. Rev.* **112** 1141
Fon W C, Berrington K A and Kingston A E 1988 *J. Phys. B: At. Mol. Opt. Phys.* **21** 2961
Henry R J W 1981 *Phys. Rep.* **68** 1
Hood S T, Weigold E and Dixon A J 1979 *J. Phys. B: At. Mol. Phys.* **12** 631
Kauppila W E, Ott W R and Fite W L 1970 *Phys. Rev.* A **1** 1099
Kingston A E, Fon W C and Burke P G 1976 *J. Phys. B: At. Mol. Phys.* **9** 605
Kingston A E and Walters H R J 1980 *J. Phys. B: At. Mol. Phys.* **13** 4633
Lloyd C R, Teubner P J O, Weigold E and Lewis B R 1974 *Phys. Rev.* A **10** 175
Long R L, Cox D M and Smith S J 1968 *J. Res. NBS* A **72** 521
Lower J, McCarthy I E and Weigold E 1987 *J. Phys. B: At. Mol. Phys.* **20** 4571

Madison D H, Hughes J A and McGinness D S 1985 *J. Phys. B: At. Mol. Phys.* **18** 2737
McCarthy I E, Ratnavelu K and Weigold A M 1988 *J. Phys. B: At. Mol. Opt. Phys.* **21** 3999
McCarthy I E, Ratnavelu K and Zhou Y 1989 *J. Phys. B: At. Mol. Opt. Phys.* **22** 2597
McCarthy I E, Saha B C and Stelbovics A T 1981 *Aust. J. Phys.* **34** 135
McCarthy I E and Stelbovics A T 1980 *Phys. Rev.* A **22** 502
—— 1983 *Phys. Rev.* A **28** 2693
Mitroy J and McCarthy I E 1989 *J. Phys. B: At. Mol. Opt. Phys.* **22** 641
Mitroy J, McCarthy I E and Stelbovics A T 1987 *J. Phys. B: At. Mol. Phys.* **20** 4827
Ochkur V I 1964 *Zh. Eksp. Teor. Fiz.* **47** 1746
Ratnavelu K 1989 *PhD* Thesis Flinders University (unpublished)
Scholz T, Scott P and Burke P G 1988 *J. Phys. B: At. Mol. Opt. Phys.* **21** L139
Stelbovics A T and Bransden B H 1989 *J. Phys. B: At. Mol. Opt. Phys.* **22** L451
Stelbovics A T and Watts R D 1982 *Flinders Institute for Atomic Studies Report* No 98 unpublished
van Wingerden B, Weigold E, de Heer F J and Nygaard K J 1977 *J. Phys. B: At. Mol. Phys.* **10** 1345
van Wyngaarden W L and Walters H R J 1986 *J. Phys. B: At. Mol. Phys.* **19** 929
Vanderpoorten R 1975 *J. Phys. B: At. Mol. Phys.* **8** 926
Walters H R J 1984 *Phys. Rep.* **116** 1
—— 1988 *J. Phys. B: At. Mol. Opt. Phys.* **21** 1893
Weigold E, Frost L and Nygaard K 1980 *Phys. Rev.* A **21** 1950
Williams J F 1974 *J. Phys. B: At. Mol. Phys.* **7** L56
—— 1975 *J. Phys. B: At. Mol. Phys.* **8** 2191
—— 1981 *J. Phys. B: At. Mol. Phys.* **14** 1197
Williams J F and Willis B A 1974 *J. Phys. B: At. Mol. Phys.* **7** L61
—— 1975 *J. Phys. B: At. Mol. Phys.* **8** 1641
Winters K H, Clark C D, Bransden B H and Coleman J P 1974 *J. Phys. B: At. Mol. Phys.* **7** 788